Central European Journal of Energetic Materials, **2015**, *12*(2), 347-357
ISSN 1733-7178
e-ISSN 2353-1843

Effects of the Burning Rate Index on the Pressure Time Profile of Progressive Burning Tubular Rocket Propellant Configurations

Himanshu SHEKHAR

High Energy Materials Research Laboratory,
Sutarwadi, Pune – 411 021, India
E-mail: himanshudrdo@rediffmail.com

Abstract: A theoretical ballistic analysis of tubular rocket propellants burning in the progressive mode was carried out with the objective of ascertaining the effects of the burning rate index on the average pressure and the total burning time of the pressure time profiles. A constant 'H' is introduced to obtain close-form expressions for the initial pressure, the maximum pressure, the area under the pressure time profile, the total burning time and the average pressure. The derivation of the total burning time for a progressive burning tubular rocket propellant is a new approach described in this paper. It is observed that the average pressure during propellant combustion varies with the burning rate index. A higher burning rate index of the propellant leads to a lower average pressure for lower burning rate propellants (8 mm/s at 7 MPa) and a higher average pressure for higher burning rate propellants (10 mm/s at 7 MPa). A unique situation occurs for an intermediate burning rate propellant (9 mm/s at 7 MPa), where the maximum pressure was obtained theoretically for a specific value of the burning rate index (0.69).

Keyword: rocket propellant, burning rate, pressure time, progressive burning, tubular configuration

1 Introduction

Solid rocket propellants burn to release thermo-chemical energy, which imparts kinetic energy for propulsion. These propellants are conceived in different configurations and are analyzed by steady state, non-transient mass balance equations. Rocket propellants are generally conceived in axis-symmetric, right circular cylindrical configurations due to the ease of manufacture and well developed ballistics. The ballistic predictions for solid sustainers (cigarette mode), tubular, multi-tubular, star port [1, 2], fin-port, finocyl [3] port, and other centrally perforated configurations [4] (funnel-port shape [5], multi-perforated [6, 7] *etc*.) have been developed for use in practical systems. Their performance prediction schemes based on a steady state as well as on transient analysis schemes have also been adequately described in the open literature. In the present article, an attempt has been made to assess the effects of the burning rate index (n) of Vieille's burning rate equation ($r = aP^n$) on the average pressure and the burning time of progressive burning tubular rocket propellant configurations using steady state ballistic equations.

2 Mathematical Formulations

Tubular propellant grains in progressive modes are utilized in ballistic evaluation motors for the characterization of propellants and the assessment of the burning rate law.

A progressive burning tubular propellant configuration is obtained by lateral and end inhibition of the configuration, and is characterized by its outer diameter (D), inner diameter (d) and length (L). The propellant burns from the inner diameter in a radially outwards direction and for a given web consumed (w), the burning surface area (S) is given by Equation 1.

$$S = \pi\,(d+2w)\,L \tag{1}$$

There is no change in the length of the propellant configuration during burning and the D of the configuration remains invariant during propellant consumption. The d expands during propellant combustion and becomes equal to the D at the end of burning. The burning surface area increases with time and attains its maximum value at the end of burning. The area under the burning surface area (S) and the web consumed (w) profile can be shown to be equal to the volume of the propellant configuration [$\int S dw = \pi L \cdot \int (d+2w)\, dw = \pi(D^2-d^2)L/4$]. Under a progressive mode of burning, the maximum available web for the complete consumption of the propellant (w_m) is given by Equation 2.

$$w_m = (D-d)/2 \tag{2}$$

The burning rate for solid rocket propellants is dependent upon pressure and it generally follows the power law given by Vieille's law. The equation is written as Equation 3, where '*n*' is called the burning rate index and has a value between 0 and 1. When the burning rate is defined at a given pressure, the burning rate coefficient (*a*) is determined with the help of the burning rate index. In fact, the burning rate index has become so engrossed in rocket propellant development that it is often treated as one of the propellant's characteristics [8-10].

$$\text{Burning rate, } r = aP^{n} \quad (3)$$

Using steady state conditions, the mass accumulation inside the rocket motor chamber is neglected and the equation for the pressure generated can be represented by Equation 4. This type of expression was derived earlier (in Ref. [4]) and is here only adapted for the progressive burning tubular rocket configuration. In this equation, the term '*H*' is a concatenated term, representing all of those parameters which do not change in the course of combustion of the propellant. The expression for *H* is given by Equation 5 and this constant is not non-dimensional in nature. The units of the variables used in the derivation of the value of *H*, affect its numerical value. The value of *H* is not independent of the burning rate index (*n*). As *n* increases, the value of *a* reduces for same burning rate (Equation 3), and the value of *H* is also lowered.

$$\text{Chamber pressure, } P = [H \times (\text{instantaneous } d)]^{1/(1-n)} \quad (4)$$

$$\text{Constant, } H = \pi a\, \rho\, C^{*}\, L\, /\, A_{t} \quad (5)$$

From Equation 4, it is clear that the initial pressure is given by $(H{\cdot}d)^{1/(1-n)}$, whilst the maximum pressure is equal to $(H{\cdot}D)^{1/(1-n)}$. The area under the pressure time profile is dependent upon the weight of propellant and the throat area. The expression is given by Equation 6. The area under the pressure time profile is independent of the burning rate index.

$$\text{Area under the pressure time profile, } \int P\mathrm{d}t = C^{*}\, W/A_{t} = H(D^{2}\text{-}d^{2})/4a \quad (6)$$

The calculation of the average pressure is a critical challenge for the calculation. In fact, if the total burning time for the complete consumption of the propellant can be obtained, then dividing the area under the pressure time profile by that burning time gives the average pressure realized during propellant consumption. One way to obtain the average pressure is from a geometrical calculation. As volume is the integration of the burning surface area over the entire web, the average burning surface area can be obtained by division of the propellant volume by the maximum web of the propellant. This burning surface area can give the average diameter of the propellant under the assumption of constant length of propellant. Using Equation 4, the value of the average pressure can be obtained. However, this method is found to be erroneous when giving the average pressure due to the significant impact of the burning rate index. For the formulation described, the average diameter of the propellant is constant for a given configuration, and, as the burning rate index increases, a higher average pressure is always realized. This is violated on several occasions, as shown by measured values as well as calculated theoretical ballistic calculations.

A more reliable way for the assessment of the average pressure is to find an equation for the total burning time of the configuration. If the total burning time (T) is known, the value of the average pressure can be obtained as the area under the pressure time profile divided by the total burning time ($P_a = \int P\mathrm{d}t/T$). The expression for the total burning time was derived as Equation 7.

$$T = \frac{1-n}{2\,a\,(1-2n)H^{\frac{n}{1-n}}}\left[D^{\frac{1-2n}{1-n}} - d^{\frac{1-2n}{1-n}}\right] for\ n \neq 0.5 \text{ and } \frac{\ln\frac{D}{d}}{2\,a\,H}\ for\ n = 0.5 \qquad (7)$$

A tubular propellant configuration with outer diameter, inner diameter and length equal to 115, 60 and 200 mm, respectively, was considered for analysis. The maximum web for the propellant configuration using Equation 2 was calculated as 27.5 mm. The propellant density and characteristic velocity were taken as 1777 kg/m^3 and 1500 m/s, respectively. The propellant weight was calculated to be 2.687 kg, which was confirmed by actual weighing of the bare propellant. The propellant burning rate at 7 MPa was evaluated as 9.6 mm/s with a burning rate index of 0.3. The propellant grain was inhibited on its lateral as well as on the end surfaces, to restrict burning on those areas. The propellant was loaded into a ballistic evaluation rocket motor and was fired with a throat diameter of 17.1 mm. The firing curve is depicted in Figure 1.

For the prediction and theoretical estimation, the mathematical formulation developed earlier was utilized. The numerical value of H was calculated to be 39.0497, using Equation 5. Using Equation 4, the initial and maximum pressure were calculated as 3.375 MPa and 8.548 MPa, for an instantaneous diameter of burning of 0.06 m and 0.115 m, respectively. The area under the pressure time profile was calculated as 17.5476 MPa·s using Equation 6. Using Equation 7, the burning time was calculated as 3.065 seconds. The average pressure was calculated to be 5.725 MPa. Numerically, the burning time from the firing curve was 3.11 s, which is comparable to the calculated burning time. The average pressure during actual firing was 5.64 MPa, against a calculated value of 5.725 MPa. The close matching of the firing curve and the prediction, in both nature and numerical values, validates the developed formulation.

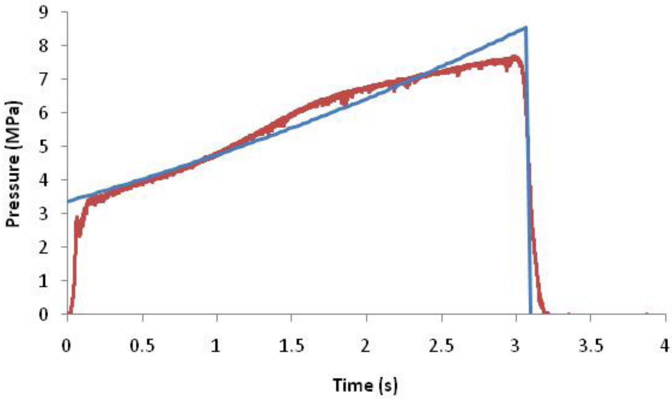

Figure 1. Pressure time profile of a static evaluation superimposed on the prediction.

3 Analysis and Discussion

For the theoretical study, the propellant dimension was considered to be the same as that evaluated in the example, earlier. The propellant density, characteristic velocity and throat diameter of rocket motor were taken as 1750 kg/m^3, 1540 m/s and 15 mm, respectively. The propellant weight was calculated to be 2.646 kg. The burning rate of the propellant was taken as 8 mm/s at 7 MPa. The value of the burning rate index was changed from 0.2 to 0.8 in increments of 0.1.

The burning area verses the web burnt profile was generated for this configuration using Equation 1. The burning area was converted into pressure using Equation 4 at each instant of the web consumed and the web consumed was converted into time using the instantaneous burning rate ($\Delta t = \Delta w/r$). The pressure time profile was obtained and is depicted in Figure 2 for three different values of the burning rate index. The figure also contains two images of the propellant, obtained at the beginning and at the end of combustion.

It is clear from the figure that a higher burning rate index gives a higher maximum pressure. However, the value of the initial pressure shows a reverse trend and is explained on the basis of the nature of the power law of burning rate in an earlier paper [11]. One of the pertinent observations is the increase in the total burning time with an increase in the burning rate index for the same burning rate. Accordingly, the value of the average pressure is also affected. The area under the pressure time profile is invariant due to the change in the burning rate index. From the curves, it is clear that a higher value of the burning rate index gives a longer burning time and lower average pressure. An increase in the burning rate index gives a steeper variation in the pressure values and an increase in the total burning time because a longer part of the propellant burns at lower pressures.

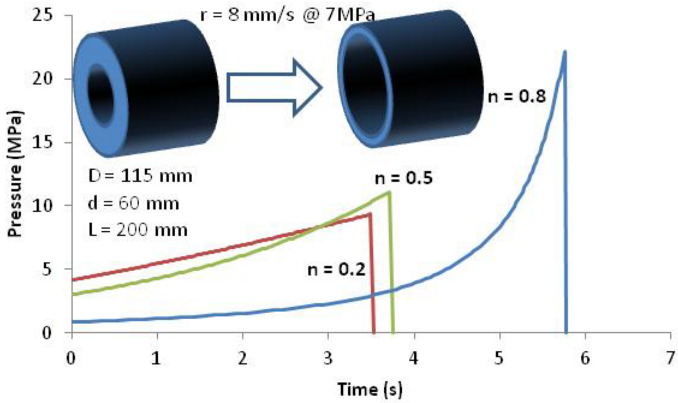

Figure 2. Pressure time profiles at different burning rate indices.

In order to observe the effect of the burning rate index on various parameters, separate curves were plotted as shown in Figure 3. The initial pressure, maximum pressure, average pressure and area under the pressure time profile are plotted on the primary axis against the burning rate index. The total burning time is plotted on the secondary axis.

The value of the area under the pressure time profile was independent of the burning rate index and was equal to 23.057 MPa·s for all of the situations. The value of the initial pressure was reduced with an increase in the burning rate index. Since the realized initial pressure is less than the pressure at which the burning rate was defined (7 MPa), a reduction in the initial pressure due to an increase in the burning rate index was obvious. For a burning rate index of 0.2, the total burning time was 3.53 s and for a burning rate index of 0.8, the total burning time was 5.78 s. Since the burning rate was defined at a pressure of 7 MPa, the time to attain 7 MPa for both the situations, was monitored. For a burning rate index of 0.2, the time to attain 7 MPa was 2.058 s, while for the other situation the time was 4.805 s. This clearly indicates that a higher burning rate index leads to a longer part of the propellant burning at lower pressures, thus reducing the average pressure, as well as increasing the total burning time. The time to burn the remaining propellant above 7 MPa is lower for a burning rate index equal to 0.8. As the burning rate index increases, the time to attain 7 MPa (pressure at which the burning rate was defined for the development of the burning rate law) increases, but the later part of the propellant is consumed at a faster pace. The combination of both depicts the total burning time and the average pressure. Since the maximum pressure is higher than the pressure at which the burning rate is defined in all of the situations, this will increase with an increase in the burning rate index. The relative variations of the initial pressure and the maximum pressure is depicted clearly in Figure 3.

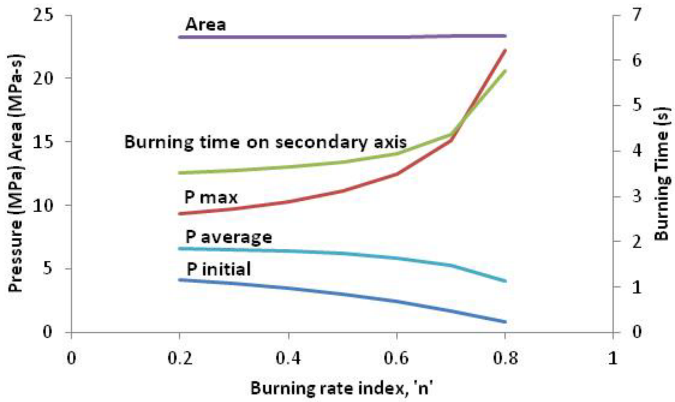

Figure 3. Variation of different parameters with burning rate index.

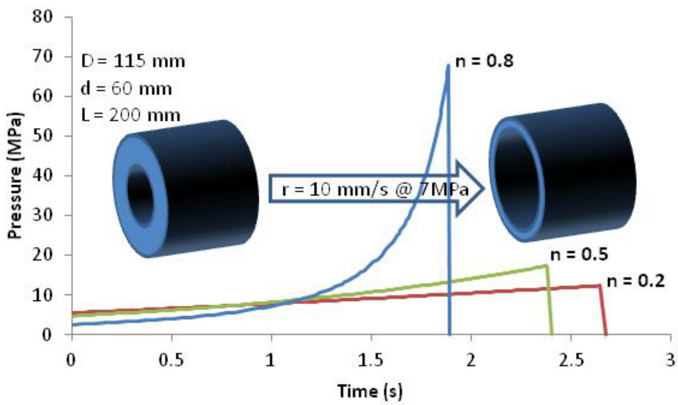

Figure 4. Effect of the burning rate index for a high burning rate propellant.

However, the variation is not universal, and to assess this, keeping all parameters constant, the burning rate of the propellant was changed to 10 mm/s at 7 MPa. The pressure time profiles for three burning rate indices are shown in Figure 4. It is observed that a higher burning rate index results in a lower total burning time for the same burning rate propellant. It is clear from the figure that the time to attain 7 MPa (pressure at which the burning rate is defined for the development of the burning rate law) is almost the same for all three situations. This makes the propellant burning at the higher pressure side a dominant factor for the assessment of the total burning time. A higher burning rate index represents a higher burning rate at a higher than specified pressure (7 MPa), giving a lower burning time. Thus the overall burning time for a higher burning rate index is lower. This indicates that a variation of the total burning time and the average pressure with burning rate index is not universal and is a function of the burning rate, too.

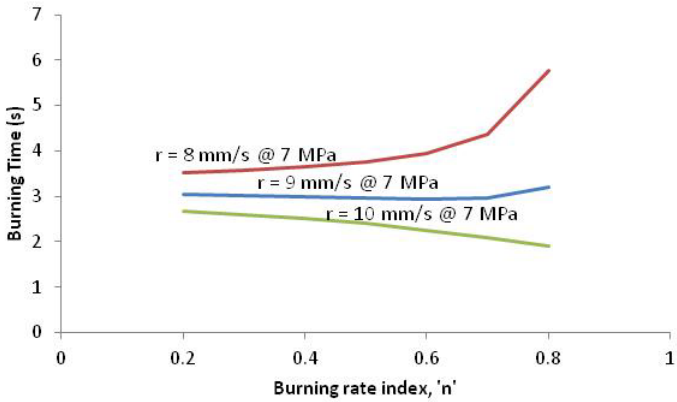

Figure 5. Variation of the burning time with burning rate index.

The variation of the total burning time with the burning rate index for different burning rate propellants is plotted in Figure 5. For all situations, the maximum web to be burnt for complete consumption of the propellant is the same. Obviously a higher burning rate propellant gives a lower burning time for the same web consumed. This is clear from Figure 5. The most important finding in the figure is the relative variation of the burning time with the burning rate index for different burning rate propellants. For a burning rate of 8 mm/s at 7 MPa, the propellant burning time increases with an increase in burning rate index. The reverse is true for a burning rate of 10 mm/s at 7 MPa. A strange type of variation is observed for a burning rate of 9 mm/s at 7 MPa. The variation of the total burning time is initially reduced up to a burning rate index of around 0.69, and is then increased. Accordingly, the average pressure will initially increase up to a burning rate index of 0.69, and then reduce. The variation of both the average pressure and the total burning time is shown in Figure 6. The total burning time (T) was calculated using Equation 7 and the average pressure was calculated using the method described in a previous section as $\int P\mathrm{d}t/T$. The curve depicted in Figure 6 gives the unique variation, where the optima for both the total burning time and the average pressure is realized at a particular value of the burning rate index.

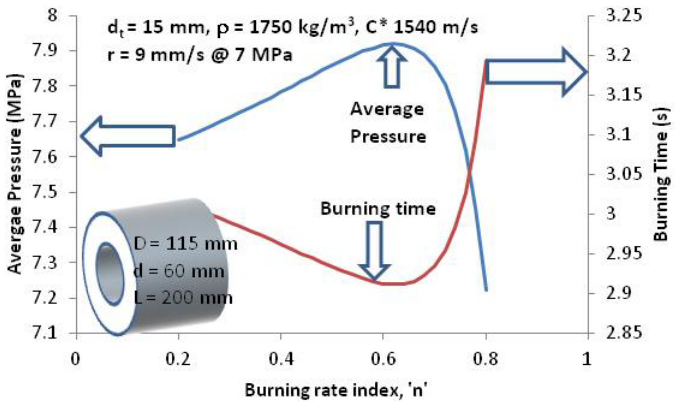

Figure 6. Variation of the burning time and the average pressure.

For a given burning rate propellant, as the burning rate index is increased, a higher variation of the pressure range is covered in progressive burning. However, this higher range is not always depicted as a higher average pressure. For lower burning rate propellants, more time is spent in attaining the pressure at which the burning rate was defined. If for the same burning rate propellant, a higher burning rate index is realized, the maximum pressure attained is higher. However, the total burning time may be longer or shorter, depending on the relative time taken by the configuration in attaining the burning rate defining pressure. The total burning time for a given burning rate propellant may be longer for both a lower burning rate index or a higher burning rate index, depending on the situation, and it is only possible to ascertain these variations by theoretical analysis. Accordingly, the average pressure, which is defined as the ratio of the area under the pressure time profile to the total burning time, has a matching variation. The entire development of a theoretical formulation is directed towards an assessment of the effect of the burning rate index on the parameters of the pressure time profiles of a progressive burning tubular rocket propellant.

4 Conclusion

A progressive burning tubular rocket propellant configuration was theoretically analyzed for its burning time and average realized pressure. The expressions for the total burning time and the average pressure were derived and the pressure time profile was analyzed. For the same burning rate propellant, the effect of the burning rate index on the average pressure is not clear. For lower burning rates, the average pressure decreases with an increase in the burning rate index, but for higher burning rate propellants, the average pressure increases with an increase in the burning rate index. In an intermediate situation, a strange case of burning rate was observed, where the average pressure is a maximum for a specific burning rate index.

Symbols:

ρ: Density of propellant (kg/m^3)
a: Burning rate coefficient
A_t : Throat area (mm^2)
C*: Characteristic velocity of propellant combustion (m/s)
d: Inner diameter of propellant (m)
D: Outer diameter of propellant (m)
H: Constant for calculation
L: Length of propellant (m)
n: Burning rate index
P: Operating chamber pressure (MPa)
r: Burning rate (m/s) = aP^n
S: Burning surface area of propellant (m^2) = π(d+2w)L
T: Total burning time (s)
w: Instantaneous web consumed (m): initially zero
W: Weight of propellant configuration (kg)
w_m : Maximum web available for consumption (m) = (D-d)/2

5 References

[1] Shekhar H., Modelling of Burning Surface Regression of Taper Convex Star Propellant Grain, *Def. Sci. J.*, **2000**, *50*(2), 207-211.
[2] Shekhar H., Parametric Studies on Star Port Propellant Grain for Ballistic Evaluations, *Def. Sci. J.*, **2005**, *55*(4), 459-469.
[3] Shekhar H., Close-form Solution for Burning Surface Evolution and Performance

Prediction of Finocyl Shaped Propellant Grain, 2007 International Autumn Seminar on Propellant, Explosives and Pyrotechnics (2007 IASPEP), Xi'an, China, **2007**, 907-911.

[4] Shekhar H., Burn Back Equations for High Volumetric Loading Single Grain Dual Thrust Rocket Propellant Configuration, *Def. Sci. J.*, **2011**, *61*(2), 165-170.

[5] Shekhar H., Design of Funnel Port Tubular Propellant Grain for Neutral Burning Profile in Rockets, *Def. Sci. J.*, **2009**, *59*(5), 494-498.

[6] Shekhar H., Design of Gas Generator Propellant Grains for Missile Applications, *Manthan – a quarterly Magazine by Bihar Brains*, **2009**, *8*, 8-11.

[7] Shekhar H., Estimation of Pressure Index and Temperature Sensitivity Coefficient of Solid Rocket Propellants by Static Evaluation, *Def. Sci. J.*, **2009**, *59*(6), 666-669.

[8] Kubota N., Aoki I., Burning Rate Characterization of GAP/HMX Energetic Composite Materials, *Propellants Explos. Pyrotech*., **2000**, *25*(4), 168-171.

[9] Babuk V.A., Dolotkazin I.N., Glebov A.A., Burning Mechanisms of Aluminized Solid Rocket Propellants Based on Energetic Binders, *Propellants Explos. Pyrotech*., **2005**, *30*(4), 281-290.

[10] Guo X., Li F., Song H., Liu G., King L., Li M., Combustion Characteristics of a Novel Grain Binding High Burning Rate Propellant, *Propellants Explos. Pyrotech*., **2008**, *33*(4), 255-260.

[11] Shekhar H., Mathematical Formulation and Validation of Muraour's Linear Burning Rate Law for Solid Rocket Propellants, *Cent. Eur. J. Energ. Mater.*, **2012**, *9*(4), 353-364.